IEEE Access
Multidisciplinary | Rapid Review | Open Access Journal

Received August 2, 2021, accepted August 8, 2021, date of publication August 18, 2021, date of current version August 30, 2021.

Digital Object Identifier 10.1109/ACCESS.2021.3105902

FxRLS Algorithms Based Active Control of Impulsive Noise With Online Secondary Path Modeling

FAREEHA JABEEN[1], ALINA MIRZA[1], AYESHA ZEB[2], MUHAMMAD IMRAN[1], FARKHANDA AFZAL[1], AND AYESHA MAQBOOL[3]

[1]MCS, National University of Sciences and Technology (NUST), Islamabad 44000, Pakistan
[2]CEME, National University of Sciences and Technology (NUST), Islamabad 44000, Pakistan
[3]NBC, National University of Sciences and Technology (NUST), Islamabad 44000, Pakistan

Corresponding author: Farkhanda Afzal (farkhanda@mcs.edu.pk)

ABSTRACT Active noise control algorithms undergo stability problems in the presence of impulsive noise. This paper investigates such algorithms with online secondary path modeling for impulsive noise and varying acoustic paths. The paper presents three methods for active noise control, along with improved online secondary path modeling. Firstly, the filtered x recursive least square algorithm is applied for both active noise control and online secondary path modeling. This method gave faster convergence, improved stability, and modeling accuracy as compared to existing ones. The filtered x recursive least square algorithm is not robust for abruptly changing acoustic paths. To overcome this problem another method that uses modified gain filtered x recursive least square algorithm for active noise control is presented. Furthermore, it is observed that modified gain filtered x recursive least square achieves the desired performance with overheads of increased complexity. Thus, a hybrid method is proposed which has less computational complexity than the rest methods with no compromise on active noise control system performance.

INDEX TERMS Active noise control, path modeling, least square algorithms, computational complexity.

I. INTRODUCTION

Active control of noise (ANC) has grown rapidly and garnered lots of consideration and attention in recent years because of the development of new successful applications using this technology [1]–[4]. The working of the ANC system is built upon the principle of superposition, i.e., generation of anti-noise signal with opposite phase but same magnitude to that of primary (unwanted) noise [4]. The filtered-x least mean square (FxLMS) algorithm is one of the most widespread, simplest, and commonly used adaptive algorithms for the ANC system [5]–[7]. The block diagram of a basic FxLMS based ANC system is shown in Fig. 1. The stability of the FxLMS algorithm needs filtering of the reference signal through the estimated secondary path [8]–[10]. Poor estimation of the secondary path i.e., when the phase response of original and estimated secondary path coefficients has a difference of more than 90 degrees, results in a low convergence rate and may cause system instability [11]. Therefore, online secondary path modeling (OSPM) methods for a feasible solution with improved efficiency of ANC system for time-varying acoustic paths are employed.

Two different approaches for OSPM are found in the literature [13]. In the first approach, additional random auxiliary noise $\mathbf{v}(\mathbf{n})$ is injected into the ANC system to employ the method of system identification for modeling of secondary path [12]–[17]. The second approach tries to model the secondary path from the output, $y(n)$ of the ANC filter without the injection of additional random noise into the ANC system [1]. The second approach does not always give an accurate secondary path estimate and its modeling process is also dependent upon the output signal. On the other hand, the first approach is not only independent of the output signal but also works fine for the entire frequency range. Therefore, the first approach is preferred in practical applications [13].

The associate editor coordinating the review of this manuscript and approving it for publication was Jinquan Xu.

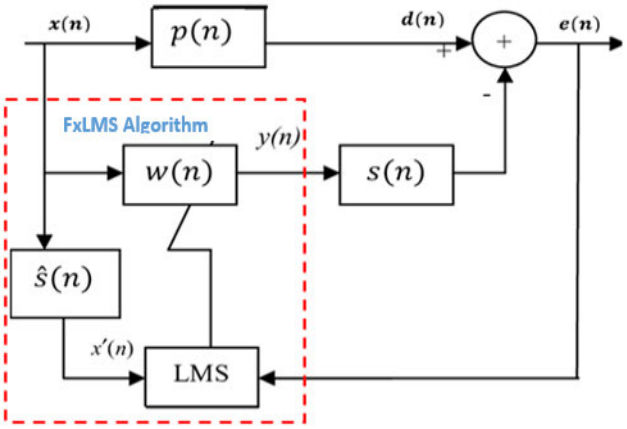

FIGURE 1. Block diagram of FxLMS algorithm-based ANC system.

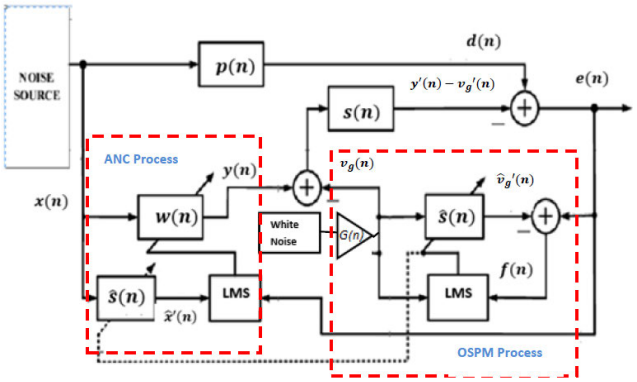

FIGURE 2. Eriksson's method for ANC systems with OSPM.

The first ANC system with OSPM was presented by Eriksson and Allie [12]. This method estimated the secondary path by introducing a random noise $v(n)$ to the system. The block diagram of [12] is shown in Fig. 2, where $\mathbf{x(n)}$ is the input reference signal, $e(n)$ is the residual error signal of the ANC filter, $\mathbf{p(n)}$ and $\mathbf{s(n)}$ are the impulse response vectors of primary and secondary acoustic paths, $\mathbf{w(n)}$ and $\hat{\mathbf{s}}\mathbf{(n)}$ represent the impulses responses of ANC and OSPM filters respectively. The description along with computations of all quantities introduced in Fig. 1 and 2, can be found in Table 1.

As seen in Fig. 2, the residual error signal of ANC filter $e\,(n)$ has two different components. One of the components i.e., $d\,(n) - y'\,(n)$ is associated with the reference signal and is beneficial for the update of the ANC filter $\mathbf{w}\,(\mathbf{n})$ but acts as a disturbance for the OSPM filter $\hat{\boldsymbol{s}}\,(\boldsymbol{n})$. The second component $v'_g\,(n)$ is related to the random noise $\mathbf{v}\,(\mathbf{n})$ and utilized in updating the modeling filter $\hat{\mathbf{s}}\,(\mathbf{n})$, but acts as a disturbance for the control filter $\mathbf{w}\,(\mathbf{n})$. Owing to this interference between the modeling and control processes, the ANC system's overall performance is degraded. To reduce this mutual interference and improve the performance of [12], numerous methods have been proposed in the literature. [13]–[16] added a third filter to reduce the cross-interference of two filters. Among these Zhang *et al.*'s method [15] gave the best reduction in mutual interference and fastest convergence

TABLE 1. Description of quantities used for the ANC systems with OSPM.

Quantity	*Description*
$\mathbf{p(n)}$	Coefficient vector of the primary path
$\mathbf{s(n)}$	Coefficient vector of the secondary path
$\hat{\mathbf{s}}\mathbf{(n)}$	Coefficient vector of OSPM filter
$\mathbf{w(n)}$	Coefficient vector of ANC filter
$\mathbf{x(n)}$	Reference / Input signal
$x'(n) = \mathbf{s(n)} * \mathbf{x(n)}$	Reference signal filtered through secondary path
$\hat{x}'(n) = \hat{\mathbf{s}}\mathbf{(n)} * \mathbf{x(n)}$	Reference signal filtered through secondary path
$d(n) = \mathbf{p(n)} * \mathbf{x(n)}$	Primary disturbance signal
$y(n) = \mathbf{w^T(n)} * \mathbf{x(n)}$	Output of ANC filter
$y'(n) = \mathbf{s(n)} * \mathbf{x(n)}$	Canceling signal
$\mathbf{v(n)}$	Auxiliary noise generated internally for OSPM filter
$G(n)$	Time-varying gain factor used for $v(n)$
$\mathbf{v_g(n)} = G(n) * \mathbf{v(n)}$	Auxiliary noise with varying gain injected into the system
$v_g'(n) = \mathbf{s(n)} * \mathbf{v_g(n)}$	Modeling signal
$\hat{v}_g'\,(n) = \hat{\mathbf{s}}\mathbf{(n)} * \mathbf{v_g(n)}$	Output of OSPM filter
$e(n) = d(n) - [y'(n) - v_g'(n)]$	Error signal of ANC filter
$f(n) = e(n) - \hat{v}_g'(n)$	Error signal of OSPM filter

in terms of overall noise reduction but at the expense of added computational complexity. In [17], Akhtar *et al.* developed an ANC system that consumed two filters, one for control and the other for modeling purposes. His variable step size FxLMS (VSS FxLMS) based OSPM filter gave faster convergence. In all these methods, the gain $G\,(n)$ of additional random noise $\mathbf{v}\,(\mathbf{n})$ was fixed i.e., $G\,(n) = 1$ (for all values of n) such that $\mathbf{v}\,(\mathbf{n}) = \mathbf{v_g}\,(\mathbf{n})$ [12]–[17]. For an efficient ANC system, $G(n)$ should approach zero as the OSPM filter approaches its steady state i.e., a good estimate of the secondary path has been achieved. If $G(n)$ is kept constant, $\mathbf{v_g(n)}$ keeps on appearing in the residual noise $e\,(n)$, resulting in overall degradation in noise reduction capability of the system. In [18], auxiliary noise power (ANP) scheduling that tracks the modeling process and then varies $G(n)$ accordingly was introduced. This ANP scheduling technique decreased the intervening of auxiliary noise $\mathbf{v_g(n)}$ in residual error $e\,(n)$ of control filter after the precise estimate of the secondary path has been achieved. In recent times, many strategies with variants of VSS FxLMS and different ANP scheduling techniques have been proposed to achieve low

residual error in steady-state, fast, and accurate modeling, and better convergence [18]–[23]. A self-tuning ANP scheduling strategy alongside the optimal VSS parameters, normalized FxLMS (VSS-FxNLMS) for both adaptive (ANC & OSPM) filters were proposed by Carini and Malatini [19]. A two-stage ANP scheduling approach was introduced by Ahmed *et al.* [21] along with a normalized variable step size algorithm for both OSPM and ANC filters. An OSPM filter equipped with VSS FxLMS and a simplified ANP scheduling strategy with decreased computational complexity was introduced by Pu *et al.* [22]. Recently, Yang *et al.* [23] have proposed an enhanced method in which the gain $G(n)$ is determined only by the modeling error $f(n)$ and the step size μ_s for the OSPM filter is adapted using the convergence of three adaptive filters. All the reported techniques [12]–[23] with OSPM focused on the modeling of the secondary path for the Gaussian noise. To the best of our awareness, no work has been reported in the literature for ANC of impulsive noise (IN) with OSPM. Therefore, in this paper, we have explored the ANC of IN along with OSPM. The IN is modeled using symmetric α-stable (SαS) model [24], which has the following characteristic function:

$$\varphi(t) = e^{-\gamma|t|^{\alpha}} \tag{1}$$

where α is called the characteristic exponent and controls the shape of distribution with value ranges $0 < \alpha \leq 2$. The nearer the value of α to 0, the heavier is the tail, which specifies the high IN. The distribution becomes Gaussian if $\alpha = 2$. In (1), the SαS distribution becomes stable SαS distribution by setting the scale parameter, γ to 1. Fig. 3 depicts SαS distribution with varying values of α.

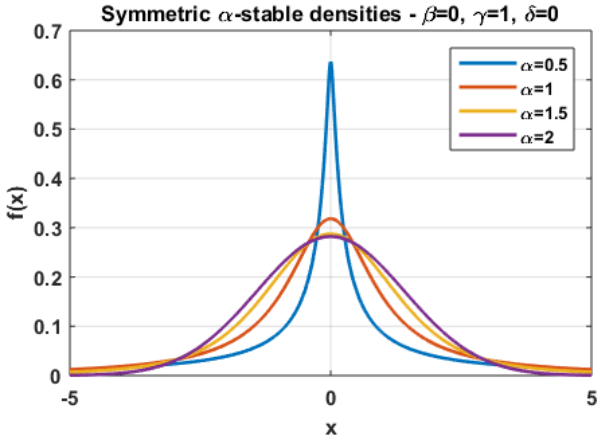

FIGURE 3. SαS distribution for varying values of α.

We tested the performance of all existing techniques in the presence of IN, given in section IV. The results validate that Carini's method [19] outperforms all other methods in the terms of noise and vibration reduction for stationary acoustic paths but diverges for a non-stationary environment. Moreover, all the reported techniques [12]–[23] used variants of FxLMS for both ANC and OSPM filters, so there is a dire need to investigate new methods for OSPM. In [25], performance comparison of FxLMS and filtered x recursive least squares (FxRLS) for ANC with IN validated the claims made in the literature that the FxRLS algorithm has superior convergence speed. These findings worked as a motivation for us to switch to the least-squares family of adaptive filters. Many novel variants of the FxRLS algorithm have also been proposed in the literature with improved performances [27]–[32], however, none of them combines online secondary path modeling with the active noise control for impulsive input. Moreover, using [26], we have incorporated the characteristic of robustness into our proposed methods too.

Therefore, three methods have been proposed in this paper were first proposed FxRLS-FxRLS method improved convergence and modeling accuracy of ANC system with OSPM, the second proposed modified gain FxRLS (MGFxRLS-FxRLS) method further improved the robustness, and the third proposed variable step size normalized FxLMS (VSS FxNLMS-FxRLS) method gave fast convergence, modeling accuracy, and robustness along with the reduced computational load. The proposed FxRLS-FxRLS method assessed the performance of the FxRLS algorithm when implemented in both ANC and OSPM filters. This method attained faster convergence than the reported variants of the FxLMS algorithm. However, the FxRLS algorithm is not much robust for non-stationary acoustic paths, and stability is not assured under high IN [2], [26]. To cater to this problem, a second proposed MGFxRLS-FxRLS method that employs the MGFxRLS algorithm [26] in ANC filter and FxRLS algorithm in OSPM filter is devised. This further improved the robustness of the overall system. However, the algorithms belonging to the FxRLS family are reported to have increased computational complexity, whereas some variants of FxLMS i.e., FxNLMS with relatively less computational complexity are found to be comparable in terms of performance with FxRLS variants [31]. These facts lead us to carry out extensive simulations and experimentations to devise our third method which not only reduced the computations but also enhanced the system performance. The proposed VSS FxNLMS-FxRLS method uses VSS FxNLMS [19] algorithm in the ANC filter and the FxRLS algorithm in the OSPM filter. The first two proposed methods i.e., the FxRLS-FxRLS method and MGFxRLS-FxRLS have been developed using the observations from the literature that validate the fast convergence of FxRLS in the presence of impulsive noise [25] and better robustness of the MGFxRLS method in a non-stationary environment [26]. However, variants of FxRLS have much higher computational complexity compared to FxLMS family algorithms [32], [33]. To overcome the issue of increased computational complexity, a novel method, i.e., the VSS FxNLMS-FxRLS algorithm, exploits the fastest convergence of FxRLS and lowers the computational complexity of the VSS FxNLMS algorithm is proposed. Henceforth, the proposed VSS FxNLMS-FxRLS method achieved superior results among

investigated [12], [18], [19], [21]–[23] and proposed techniques for the active cancellation of impulsive noise with online secondary path modeling.

The rest of this paper is structured as follows: The proposed methods are discussed in Section 2. The complexity analysis of proposed methods is given in Section 3 followed by the comparative analysis of proposed and existing methods with the help of simulation experiments in Section 4. Finally, a conclusion is drawn in Section 5.

II. PROPOSED METHODS

In this section, we present the proficient methods for the OSPM with ANC of IN. Three suggested algorithms are discussed below.

A. PROPOSED FxRLS ALGORITHM BASED ANC AND OSPM (FxRLS-FxRLS METHOD)

The block diagram of the proposed FxRLS-FxRLS method is given in Fig. 4. All the existing techniques for OSPM worked fine with Gaussian input but were not very efficient in terms of modeling accuracy and convergence in the presence of IN. Moreover, many of these methods [12], [14]–[23] lacked robustness for varying acoustic paths. Therefore, we have proposed a method where both ANC and OSPM filters employ the FxRLS algorithm. FxRLS algorithm minimizes the sum of square error by recursively finding the filter coefficients [32].

The weights of the OSPM filter are updated as:

$$\hat{\mathbf{s}}\,(\mathbf{n}+\mathbf{1}) = \hat{\mathbf{s}}\,(\mathbf{n}) + \mathbf{k_2}\,(\mathbf{n}) f\,(n) \tag{2}$$

where

$$\mathbf{k_2}\,(\mathbf{n}) = \frac{\mathbf{P_2}\,(\mathbf{n}-\mathbf{1})\,\boldsymbol{v_g}(\mathbf{n})}{\mathbf{v_g^T}\,(\mathbf{n})\,\mathbf{P_2}\,(\mathbf{n}-\mathbf{1})\,\mathbf{v_g}\,(\mathbf{n})+\lambda} \tag{3}$$

$$f\,(n) = [d\,(n) - y\,(n)] + \left[v_g'(n) - \hat{v}_g'(n)\right] \tag{4}$$

$\mathbf{k_2}$ in (4) is the gain used to predict weights of modeling filter with decreasing modeling error $f(n)$, λ is forgetting factor with value ranges between 0.9-1 and $\boldsymbol{P_2}$ is the covariance matrix of $\mathbf{v_g}\,(\mathbf{n})$ which is updated as:

$$\mathbf{P_2}\,(\mathbf{n}) = \lambda^{-1}\mathbf{P_2}\,(\mathbf{n}-\mathbf{1}) - \lambda^{-1}\mathbf{k_2}\,(\mathbf{n})\,\mathbf{v_g^T}\,(\mathbf{n})\,\mathbf{P_2}\,(\mathbf{n}-\mathbf{1}) \tag{5}$$

The ANC filter update equation is provided as:

$$\mathbf{w}\,(\mathbf{n}+\mathbf{1}) = \mathbf{w}\,(\mathbf{n}) + \mathbf{k_1}\,(\mathbf{n})\,e\,(n) \tag{6}$$

where

$$\mathbf{k_1}\,(\mathbf{n}) = \frac{\mathbf{P_1}\,(\mathbf{n}-\mathbf{1})\,\hat{\mathbf{x}}'\,(\mathbf{n})}{\hat{\mathbf{x}}'^{\mathbf{T}}\,(\mathbf{n})\,\mathbf{P_1}\,(\mathbf{n}-\mathbf{1})\,\hat{\mathbf{x}}'\,(\mathbf{n})+\lambda} \tag{7}$$

$$\mathbf{P_1}\,(\mathbf{n}) = \lambda^{-1}\mathbf{P_1}\,(\mathbf{n}-\mathbf{1}) - \lambda^{-1}\mathbf{k_1}\,(\mathbf{n})\,\hat{\mathbf{x}}'^{\,\mathbf{T}}\,(\mathbf{n})\,\mathbf{P_1}\,(\mathbf{n}-\mathbf{1}) \tag{8}$$

As mentioned earlier, $v_g'(n)$ serves as a disturbance in $e(n)$. If the gain of auxiliary noise is kept constant, this will cause a continuous degradation in the ANC filter. To overcome this problem, the ANP scheduling approach was presented in [18]. According to this, once the OSPM filter has attained a steady state, the gain of auxiliary noise should be significantly

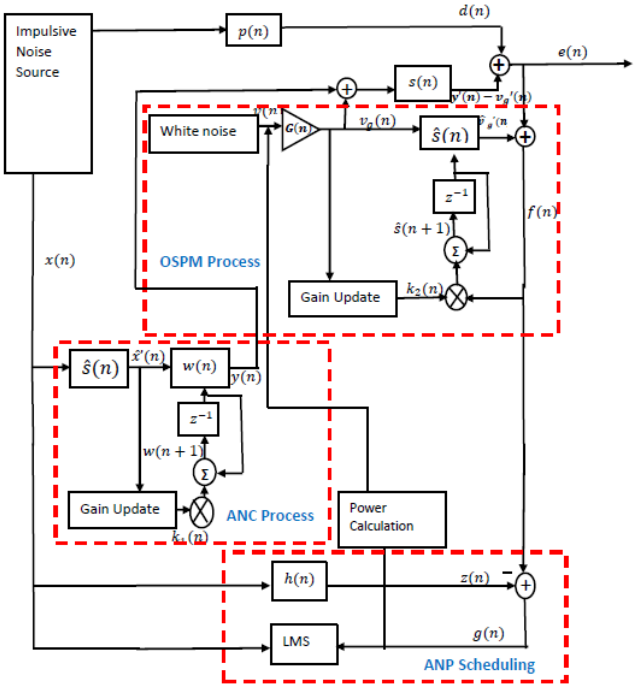

FIGURE 4. Block diagram of the proposed FxRLS – FxRLS method.

reduced until a change in the secondary path is encountered. ANP scheduling used in this paper is the same as in [23]. The gain $G(n)$ for all investigated methods is updated as:

$$G\,(n) = c\sqrt{P_g(n)} \tag{9}$$

where

$$P_g\,(n) = \lambda P_g\,(n-1) + (1-\lambda)\,g^2\,(n) \tag{10}$$

A third filter $\mathbf{h}(\mathbf{n})$ is used for the power calculation $P_g(n)$. This filter is updated as:

$$\mathbf{h}\,(\mathbf{n}+\mathbf{1}) = \mathbf{h}\,(\mathbf{n}) + \mu_h g\,(n)\,\mathbf{x}\,(\mathbf{n}) \tag{11}$$

The value of $G(n)$ keeps on decreasing as OSPM filter coefficients approach the actual secondary path-vector ensuring improved modeling accuracy of the system. If a sudden change is encountered in the secondary path, $G(n)$ again becomes large, hence increasing the amplitude of $\mathbf{v_g}(\mathbf{n})$. The faster the OSPM filter converges, the lesser is the value of $f(n)$ and lower is the contribution of $\mathbf{v_g}(\mathbf{n})$ in $e(n)$. With the use of the FxRLS algorithm along with ANP scheduling not only the ANC filter's performance is enhanced but the OSPM filter also attains the accurate model of the secondary path in minimum time.

However, for non-stationary acoustic paths, re-initialization needs to be done for FxRLS which is very difficult rather impossible in the course of runtime application [34]. Practically, for varying acoustic paths, the FxRLS algorithm is deficient in robustness and may even become unstable. Thus, modifications are obligatory in the proposed FxRLS-FxRLS method to make it robust. In the next section, we proposed the MGFxRLS-FxRLS method. MGFxRLS is reported in

the literature to have better robustness for the non-stationary environment [26]. Hence method 2 not only preserves the fast converging property of method 1 but is also robust in the presence of changing acoustic paths.

B. PROPOSED MGFxRLS ALGORITHM BASED ANC AND FxRLS ALGORITHM BASED OSPM (MGFxRLS-FxRLS METHOD)

In this proposed method, the ANC filter uses the MGFxRLS algorithm whereas the OSPM filter employs FxRLS. The OSPM filter employs the FxRLS algorithm and is updated as:

$$\hat{\mathbf{s}}(\mathbf{n}+\mathbf{1}) = \hat{\mathbf{s}}(\mathbf{n}) + \mathbf{k_2}(\mathbf{n}) f(n) \tag{12}$$

where

$$\mathbf{k_2}(\mathbf{n}) = \frac{\mathbf{P_2}(\mathbf{n}-\mathbf{1})\,\mathbf{v_g}(\mathbf{n})}{\mathbf{v_g^T}(\mathbf{n})\,\mathbf{P_2}(\mathbf{n}-\mathbf{1})\,\mathbf{v_g}(\mathbf{n}) + \lambda} \tag{13}$$

$\mathbf{k_2}$ is the gain and $\mathbf{P_2}$ is the covariance matrix of $\mathbf{v_g(n)}$ which is updated as:

$$\mathbf{P_2}(\mathbf{n}) = \lambda^{-1}\mathbf{P_2}(\mathbf{n}-\mathbf{1}) - \lambda^{-1}\mathbf{k_2}(\mathbf{n})\,\mathbf{v_g}^{\mathbf{T}}(\mathbf{n})\,\mathbf{P_2}(\mathbf{n}-\mathbf{1}) \tag{14}$$

The ANC filter is based on the MGFxRLS algorithm. The weights ANC filter have the following update equation:

$$\mathbf{w}(\mathbf{n}+\mathbf{1}) = \mathbf{w}(\mathbf{n}) + \mathbf{k_1}(\mathbf{n})\, e(n) \tag{15}$$

where

$$\mathbf{k_1}(\mathbf{n}) = \frac{\mathbf{P_1}(\mathbf{n}-\mathbf{1})\,\hat{\mathbf{x}}'(\mathbf{n})}{\hat{\mathbf{x}}'^{\mathbf{T}}(\mathbf{n})\,\mathbf{P_1}(\mathbf{n}-\mathbf{1})\,\hat{\mathbf{x}}'(\mathbf{n}) + \lambda + E_e(n)} \tag{16}$$

$$\mathbf{P_1}(\mathbf{n}) = \lambda^{-1}\mathbf{P_1}(\mathbf{n}-\mathbf{1}) - \lambda^{-1}\mathbf{k_1}(\mathbf{n})\,\hat{\mathbf{x}}'^{\mathbf{T}}(\mathbf{n})\,\mathbf{P_1}(\mathbf{n}-\mathbf{1}) \tag{17}$$

$$E_e(n) = \lambda E_e(n-1) + (1-\lambda)\left|e^2(n)\right| \tag{18}$$

$E_e(n)$ is the energy of the residual error $e(n)$ and $\mathbf{P_1}$ is the covariance matrix of $\hat{x}'(n)$. The gain $G(n)$ is updated as:

$$G(n) = c\sqrt{P_g(n)} \tag{19}$$

where

$$P_g(n) = \lambda P_g(n-1) + (1-\lambda)\, g^2(n) \tag{20}$$

A third filter $\mathbf{h(n)}$ is used for the power calculation $P_g(n)$. This filter is updated as:

$$\mathbf{h}(\mathbf{n}+\mathbf{1}) = \mathbf{h}(\mathbf{n}) + \mu_h g(n)\,\mathbf{x}(\mathbf{n}) \tag{21}$$

Simulation results in Section IV authenticate the improved robustness of the proposed MGFxRLS-FxRLS method. If the acoustic paths change, the proposed MGFxRLS-FxRLS method still shows good convergence along with the low steady-state error, hence, ensuring robustness and stability of this algorithm. However, it is important to mention here that although both proposed FxRLS-FxRLS and proposed MGFxRLS-FxRLS methods give good noise reduction, faster convergence, and good modeling accuracy but at the cost of increased computational complexity. This motivated us to devise our third hybrid method which not only gives reduced computations but also enhances the system's overall performance. This method is presented in the next section.

C. PROPOSED VSS FxNLMS ALGORITHM BASED ANC AND FxRLS ALGORITHM BASED OSPM-(VSS FxNLMS-FxRLS METHOD)

We suggest a new method for OSPM that combines the high convergence speed and good modeling accuracy features of the FxRLS algorithm with the noise reduction capability of the VSS FxNLMS algorithm. The FxNLMS algorithm with optimal VSS derived in [19] is found to be most efficient in terms of noise reduction when used in an ANC filter. The proposed VSS FxNLMS-FxRLS method uses the VSS FxNLMS algorithm [19] in the ANC filter and the FxRLS algorithm in the OSPM filter. The block diagram of this method is given in Fig. 5.

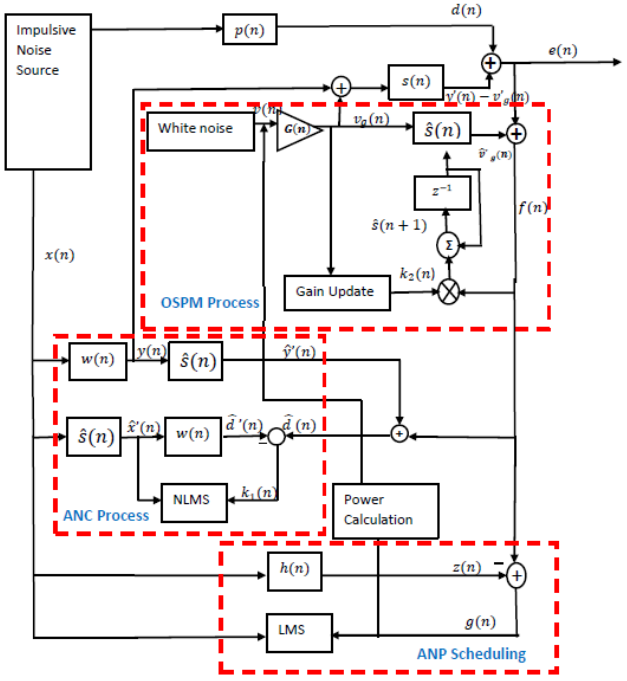

FIGURE 5. Block diagram of the proposed VSS FxNLMS – FxRLS method.

The weight update equation of the ANC filter is given as:

$$\mathbf{w}(\mathbf{n}+\mathbf{1}) = \mathbf{w}(\mathbf{n}) + \mu_w(n)\,\frac{\mathbf{k_1}(\mathbf{n})\,\hat{\mathbf{x}}'(\mathbf{n})}{\hat{\mathbf{x}}'^{\mathbf{T}}(\mathbf{n})\,\hat{\mathbf{x}}'(\mathbf{n})} \tag{22}$$

The step size parameter of the ANC filter $\mu_w(n)$ is approximated using the following equation:

$$\mu_w(n) = \frac{\hat{N}_w(n)}{P_e(n)} \tag{23}$$

where

$$\hat{N}_w(n) = \lambda\hat{N}_w(n-1) + (1-\lambda)\, e(n)\,\hat{\mathbf{m}}^{\mathbf{T}}(\mathbf{n})\,\hat{\mathbf{x}}'(\mathbf{n}) \tag{24}$$

TABLE 2. Computational complexity analysis of proposed FxRLS-FxRLS method.

For each n calculate	*	+/-	/	√
$G(n) = c\sqrt{P_g(n)}$	1			1
$\mathrm{v_g(n)} = G(n)\mathbf{v(n)}$	1			
$v_g'(n) = \mathrm{s^T(n)v_g(n)}$	M	M-1		
$\hat{x}'(n) = \hat{\mathbf{s}}^{\mathbf{T}}(\mathbf{n})\mathbf{x}(\mathbf{n})$	M	M-1		
$y(n) = \mathbf{w}^{\mathbf{T}}(\mathbf{n})\mathbf{x}(\mathbf{n})$	L_w	L_w -1		
$y'(n) = \mathbf{s}^{\mathbf{T}}(\mathbf{n})y(n)$	M	M-1		
$\hat{v}_g'(n) = \hat{\mathbf{s}}^{\mathbf{T}}(\mathbf{n})\,\mathbf{v_g}(\mathbf{n})$	M	M-1		
$e(n) = d(n) - [y'(n) - v_g'(n)]$		2		
$f(n) = e(n) - \hat{v}_g'(n)$		1		
$z(n) = \mathbf{h}^{\mathbf{T}}(\mathbf{n})\boldsymbol{x}(\boldsymbol{n})$	K	K-1		
$g(n) = f(n) - z(n)$		1		
$P_g(n) = \lambda P_g(n-1) + (1-\lambda)\,g^2(n)$	3	2		
$\mathbf{P_2(n)} = \lambda^{-1}\mathbf{P_2(n-1)} - \lambda^{-1}\mathbf{k_2(n)v_g}^{\mathbf{T}}\mathbf{(n)P_2(n-1)}$	3 $L_w{}^2$	2 $L_w{}^2$- L_w	1	
$\mathbf{P_1(n)} = \lambda^{-1}\mathbf{P_1(n-1)} - \lambda^{-1}\mathbf{k_1(n)}\hat{\mathbf{x}}'\mathbf{(n)P_1(n-1)}$	$3M^2$	$2M^2$-M	1	
$\mathbf{k_2(n)} = \dfrac{\mathbf{P_2(n-1)v_g(n)}}{\boldsymbol{v_g}^{T}(n)\mathbf{P_2(n-1)v_g(n)} + \lambda}$	$2M$	M	1	
$\mathbf{k_1(n)} = \dfrac{\mathbf{P_1(n-1)}\hat{\mathbf{x}}'\mathbf{(n)}}{\hat{\mathbf{x}}'^{\mathbf{T}}\mathbf{(n)P_1(n-1)}\hat{\mathrm{x}}'\mathrm{(n)} + \lambda}$	2 L_w	L_w	1	
$\hat{\mathbf{s}}(\mathbf{n+1}) = \hat{\mathbf{s}}(\mathbf{n}) + \mathbf{k_2(n)}\,f(n)$	M	M		
$\mathbf{w(n+1)} = \mathbf{w(n)} + \mathbf{k_1(n)}\,e(n)$	L_w	L_w		
$\mathbf{h(n+1)} = \mathbf{h(n)} + \mu_h g(n)\,\mathbf{x(n)}$	K+1	K		
Total Computations in proposed FxRLS-FxRLS method :	$3M^2$+7M+3 $L_w{}^2$+ 4 L_w +2K+5	$2M^2$+5M+2 $L_w{}^2$+ 2 L_w +2K-2	4	1

$$\hat{\mathbf{m}}(\mathbf{n}) = \hat{\lambda}\hat{\mathbf{m}}(\mathbf{n-1}) + (1-\hat{\lambda})\frac{g(n)\hat{\boldsymbol{x}}'(\mathbf{n})}{\hat{\mathbf{x}}'(\mathbf{n})^{\mathbf{T}}\hat{\mathbf{x}}'(\mathbf{n})} \tag{25}$$

$$P_e(n) = \lambda P_e(n-1) + (1-\lambda)\,e^2(n) \tag{26}$$

The weight update equation of the OSPM filter is specified as:

$$\hat{\mathbf{s}}(\mathbf{n+1}) = \hat{\mathbf{s}}(\mathbf{n}) + \mathbf{k_2}(\mathbf{n})f(n) \tag{27}$$

where

$$\mathbf{k_2}(\mathbf{n}) = \frac{\mathbf{P_2}(\mathbf{n-1})\,\mathbf{v_g}(\mathbf{n})}{\mathbf{v_g^T}(\mathbf{n})\,\mathbf{P_2}(\mathbf{n-1})\,\mathbf{v_g}(\mathbf{n}) + \lambda} \tag{28}$$

$$\mathbf{P_2}(\mathbf{n}) = \lambda^{-1}\mathbf{P_2}(\mathbf{n-1}) - \lambda^{-1}\mathbf{k_2}(\mathbf{n})\,\mathbf{v_g^T}(\mathbf{n})\,\mathbf{P_2}(\mathbf{n-1}) \tag{29}$$

Gain is updated as:

$$G(n) = c\sqrt{P_g(n)} \tag{30}$$

TABLE 3. Computational complexity analysis of proposed MGFxRLS-FxRLS method.

For each n calculate	*	+/-	/	√
$G(n) = c\sqrt{P_g(n)}$	1			1
$\mathbf{v_g(n)} = G(n)\mathbf{v(n)}$	1			
$v_g'(n) = \mathbf{s^T(n)}\boldsymbol{v_g}(n)$	M	M-1		
$\hat{x}'(n) = \mathbf{\hat{s}^T(n)x(n)}$	M	M-1		
$y(n) = \mathbf{w^T(n)x(n)}$	L_w	L_w -1		
$y'(n) = \mathbf{s^T(n)}y(n)$	M	M-1		
$\hat{v}_g'(n) = \mathbf{\hat{s}^T(n)\ v_g(n)}$	M	M-1		
$e(n) = d(n) - [y'(n) - v_g'(n)]$		2		
$f(n) = e(n) - \hat{v}_g'(n)$		1		
$z(n) = \mathbf{h^T(n)x(n)}$	K	K-1		
$g(n) = f(n) - z(n)$		1		
$P_g(n) = \lambda P_g(n-1) + (1-\lambda)\, g^2(n)$	3	2		
$\mathbf{P_2(n)} = \lambda^{-1}\mathbf{P_2(n-1)} - \lambda^{-1}\mathbf{k_2(n)}\mathrm{v_g^T(n)P_2(n-1)}$	3 $L_w{}^2$	2 $L_w{}^2$- L_w	1	
$\mathbf{P_1(n)} = \lambda^{-1}\mathbf{P_1(n-1)} - \lambda^{-1}\mathbf{k_1(n)\hat{x}'(n)P_1(n-1)}$	$3M^2$	$2M^2$-M	1	
$\mathbf{k_2(n)} = \frac{\mathbf{P_2(n-1)v_g(n)}}{v_g^T(n)\mathbf{P_2(n-1)v_g(n)}+\lambda}$	$2M$	M	1	
$E_e(n) = \lambda E_e(n-1) + (1-\lambda)\lvert e^2(n)\rvert$	3	2		
$\mathbf{k_1(n)} = \frac{\mathbf{P_1(n-1)\hat{x}'(n)}}{\mathbf{\hat{x}'^T(n)P_1(n-1)\hat{x}'(n)}+\lambda+Ee(n)}$	2 L_w	L_w+1	1	
$\mathbf{\hat{s}(n+1)} = \mathbf{\hat{s}(n)} + \mathbf{k_2(n)}\, f(n)$	M	M		
$\mathbf{w(n+1)} = \mathbf{w(n)} + \mathbf{k_1(n)}\, e(n)$	L_w	L_w		
$\mathbf{h(n+1)} = \mathbf{h(n)} + \mu_h g(n)\, \mathbf{x(n)}$	K+1	K		
Total Computations in proposed MGFxRLS-FxRLS method:	$3M^2$+7M+3$L_w{}^2$+ 4 L_w +2K+8	$2M^2$+5M+2$L_w{}^2$+ 2 L_w +2K+1	4	1

$$P_g(n) = \lambda P_g(n-1) + (1-\lambda)\, g^2(n) \tag{31}$$

The third filter $\mathbf{h(n)}$ used for the power calculation $P_g(n)$ is updated as:

$$\mathbf{h(n+1)} = \mathbf{h(n)} + \mu_h g(n)\, \mathbf{x(n)} \tag{32}$$

Simulation results have validated our claim that the proposed VSS FxNLMS-FxRLS method has enhanced robustness, stability, and convergence with reduced computations in comparison to other existing and proposed methods.

III. COMPUTATIONAL COMPLEXITY

Computational complexity plays a vital role in the implementation of algorithms in real-time applications. The proposed methods' complexity per iteration is specified in Tables 2-4, respectively. The computational complexity of existing and proposed methods is given in Table 5.

TABLE 4. Computational complexity analysis of proposed VSS FxNLMS-FxRLS method.

For each n calculate	*	+/-	/	√
$G(n) = c\sqrt{P_g(n)}$	1			1
$v_g(n) = G(n)\mathbf{v(n)}$	1			
$v_g'(n) = \mathbf{s^T(n)v_g(n)}$	M	M-1		
$\hat{v}_g'(n) = \mathbf{\hat{s}^T(n)\,v_g(n)}$	M	M-1		
$y(n) = \mathbf{w^T(n)} * \mathbf{x(n)}$	L_w	L_w-1		
$y'(n) = \mathbf{s^T(n)} * y(n)$	M	M-1		
$\hat{y}'(n) = \mathbf{\hat{s}^T(n)} * y(n)$	M	M-1		
$\hat{x}'(n) = \mathbf{\hat{s}^T(n)} * \mathbf{x(n)}$	M	M-1		
$f(n) = e(n) - \hat{v}_g'(n)$		1		
$\hat{d}'(n) = \mathbf{w^T(n)} * \mathbf{\hat{x}'(n)}$	L_w	L_w-1		
$\hat{d}(n) = \hat{y}'(n) + f(n)$		1		
$k_1(n) = \hat{d}(n) - \hat{d}'(n)$		1		
$z(n) = \mathbf{h^T(n)} * \mathbf{x(n)}$	K	K-1		
$g(n) = f(n) - z(n)$		1		
$P_g(n) = \lambda P_g(n-1) + (1-\lambda)\, g^2(n)$	3	2		
$P_e(n) = \lambda P_e(n-1) + (1-\lambda)\, e^2(n)$	3	2		
$\mathbf{P(n)} = \lambda^{-1}\,\mathbf{P(n-1)k_2(n)} - \lambda^{-1}\mathbf{k_2(n)}v_g^T(n)\,\mathbf{P(n-1}$	$3M^2$	$2M^2$-M	1	
$\mathbf{k_2(n)} = \frac{\mathbf{P(n-1)v_g(n)}}{\mathbf{v_g}^T\mathbf{(n)\,P(n-1)v_g(n)}+\lambda}$	$2M$	M+1	1	
$\mathbf{\hat{m}(n)} = \hat{\lambda}\mathbf{\hat{m}(n-1)} + \left(1-\hat{\lambda}\right)\frac{\mathbf{k_2(n)\hat{x}\prime(n)}}{\mathbf{\hat{x}'^T(n)\hat{x}\prime(n)}}$	$2L_w$+1	L_w	1	
$\hat{N}_w(n) = \lambda\,\hat{N}_w(n-1) + (1-\lambda)\mathbf{k_2(n)\hat{m}^T(n)\hat{x}'(n)}$	L_w+2	L_w		
$\mu_w(n) = \frac{\hat{\hat{N}}_w(n)}{P_e(n)}$	1			
$\mathbf{\hat{s}(n+1)} = \mathbf{\hat{s}(n)} + \mathbf{k_2(n)}\, f(n)$	M	M		
$\mathbf{w(n+1)} = \mathbf{w(n)} + \mu_w(n)\frac{k_1(n)\mathbf{\hat{x}'(n)}}{\mathbf{\hat{x}'^T(n)\hat{x}'(n)}}$				
$\mathbf{h(n+1)} = \mathbf{h(n)} + \mu_h g(n)\,\mathbf{x(n)}$	K+1	K		
Total Computations in proposed VSS FxNLMS-FxRLS method:	$3M^2$+ $8M$+$5L_w$+ $2K$+9	$2M^2$+$6M$+$4L_w$+$2K$ +1	3	1

TABLE 5. Computational complexity analysis of the proposed and several existing methods.

Methods	*,/,√	+,-	Total
Carini's method [19]	$7L_w$+6M+4D+26	$6L_w$+6M+4D-1	$13L_w$+12M+8D+25
Ahmed's method [21]	$5L_w$+9M+36	$5L_w$+9M+6	$10L_w$+18M+42
Pu's method [22]	$2L_w$+3M+18	$2L_w$+3M+3	$4L_w$+4M+21
Yang's method [23]	$2L_w$+3M+2K+19	$2L_w$+3M+2K+5	$4L_w$+6M+4K+24
Proposed FxRLS-FxRLS method	$3M^2$+7M+$3L_w^2$+ $4L_w$+2K+10	$2M^2$+5M+$2L_w^2$+ $2L_w$+2K-2	$5M^2$+12M+$5L_w^2$+$6L_w$+4K +8
Proposed MGFxRLS-FxRLS method	$3M^2$+7M+$3L_w^2$+ $4L_w$+2K+13	$2M^2$+5M+$2L_w^2$+ $2L_w$+2K+1	$5M^2$+12M+$5L_w^2$+$6L_w$+4K +14
Proposed VSS FxNLMS-FxRLS method	$3M^2$+ 8M+$5L_w$+2K +13	$2M^2$+6M+$4L_w$+2K+1	$5M^2$+14M+$9L_w$+4K+14

TABLE 6. Set of parameters fixed for all simulations.

ANC System with OSPM			**Impulsive Noise *x(n)***		
Parameter	Symbol	Value	Parameter	Symbol	Value
Primary path tap length	L	48	Total Realizations	Avg	10
Secondary path tap length	M	16	Total Iterations	N	100,000
ANC filter tap length	L_w	32	Characteristic exponent	α	1.65, 1.85
			Scale Parameter	γ	1
			Location Parameter	C	0
OSPM filter tap length	M	16	Skewness parameter	δ	0

In Table 2-5, L_w, K, M, and D represent the number of filter coefficients of $\mathbf{w}(\mathbf{n})$, $\mathbf{h}(\mathbf{n})$, $\hat{\mathbf{s}}(\mathbf{n})$ and delay used in [19], respectively. It is a well-developed fact in the literature that the FxRLS algorithm and its variants have much higher computational complexities although they have exemplary performances and hence our proposed FxRLS-FxRLS method and proposed MGFxRLS-FxRLS method also have increased complexity. To reduce the complexity of these methods without compromising performance, the VSS FxNLMS-FxRLS method has been proposed. Fig. 6 (a-c) shows the comparison of computations involved in all investigated [19], [21]–[23] and proposed methods. Fig. 6 (a-b) shows a comparison of the number of additions and multiplications involved in various proposed and investigated methods, whereas, Fig. 6 (c), shows an assessment of total computations taking place in each method. From Fig. 6 (a-c), it is evident that the computational complexity of the proposed VSS FxNLMS-FxRLS method is much reduced and comparable to existing algorithms [19], [21]–[23]. Moreover, the performance of the proposed VSS FxNLMS-FxRLS method is much better.

IV. SIMULATION RESULTS

This section provides and discusses simulation results of various experiments carried out using MATLAB and also delivers a detailed comparative analysis of existing and proposed methods for ANC of IN with OSPM. The following existing methods are compared with the proposed methods:

- Erikson's method [12]
- Akhtar's method [18]
- Carini's method [19]
- Ahmad's method [21]
- Pu's method [22]
- Yang's method [23]

The comparison of the investigated algorithms is carried out based on the following three performance metrics:

i Mean Noise Reduction, *MNR* is calculated as:

$$\Delta MNR(n) = E\left\{\frac{A_e(n)}{A_d(n)}\right\} \tag{33}$$

$$A_e(n) = \lambda A_e(n-1) + (1-\lambda)|e(n)| \tag{34}$$

$$A_d(n) = \lambda A_d(n-1) + (1-\lambda)|d(n)| \tag{35}$$

where $A_d(n)$ and $A_e(n)$ (n)represent the absolute values of disturbance and residual error signal respectively.

ii Vibration reduction, R is computed as:

$$R(n) = -10\log\left\{\frac{\sum e(n)^2}{\sum d(n)^2}\right\} \tag{36}$$

iii Relative modeling error of secondary path, Δ S is given by:

$$\Delta S(n) = 10\log_{10}\frac{\left\|\mathbf{s}(\mathbf{n}) - \hat{\mathbf{s}}(\mathbf{n})\right\|^2}{\|\mathbf{s}(\mathbf{n})\|^2} \tag{37}$$

The primary $\mathbf{p}(\mathbf{n})$ and secondary $\mathbf{s}(\mathbf{n})$ acoustic paths are modeled as FIR filters by means of data taken from [1]. The impulse response of both acoustic paths is truncated to memory lengths of 48 and 16, respectively, and is depicted in Fig. 7(a-b). The tap length of ANC filter $\mathbf{w}(\mathbf{n})$ and OSPM filter $\hat{\mathbf{s}}(\mathbf{n})$ is set to 32 and 16, respectively for all the investigations in this paper.

Two phases of the ANC system have been taken into account as in [19] for all simulations in this paper. In the first phase, the ANC filter is kept inactive till 5000 iterations and only the OSPM filter is adapted to obtain the secondary path's initial estimate. In the second phase, after 5000 iterations the system is operated by adapting both OSPM and ANC filters simultaneously. Therefore, in all plots of this section, the vertical dashed line at $n = 5000$ denotes the end of the inactive ANC phase. The auxiliary signal $\mathbf{v}(\mathbf{n})$ is white Gaussian noise with zero mean and 0.05 variance. Exhaustive examinations have been performed to get the fitting value of parameters for the efficient OSPM performance of the ANC system. The parameters used in simulating the ANC with OSPM for IN are listed in Table 6. In the simulations of the ANC system, three cases are considered:

Case 1: Moderate impulsive input ($\alpha = 1.85$) with stationary acoustic paths.

Case 2: Moderate Impulsive input ($\alpha = 1.85$) with non-stationary acoustic paths.

Case 3: High Impulsive input ($\alpha = 1.65$) with non-stationary acoustic paths.

A. CASE 1: MODERATE IMPULSIVE INPUT ($\alpha = 1.85$) WITH STATIONARY ACOUSTIC PATHS

In case 1, the performance of already reported algorithms [12], [18]–[23] for ANC of IN with OSPM is tested when the input is impulsive ($\alpha = 1.85$) in nature and acoustic paths are also stationary. Extensive simulations are executed to find the suitable values of various controlling parameters of all existing methods which are listed in Table 7.

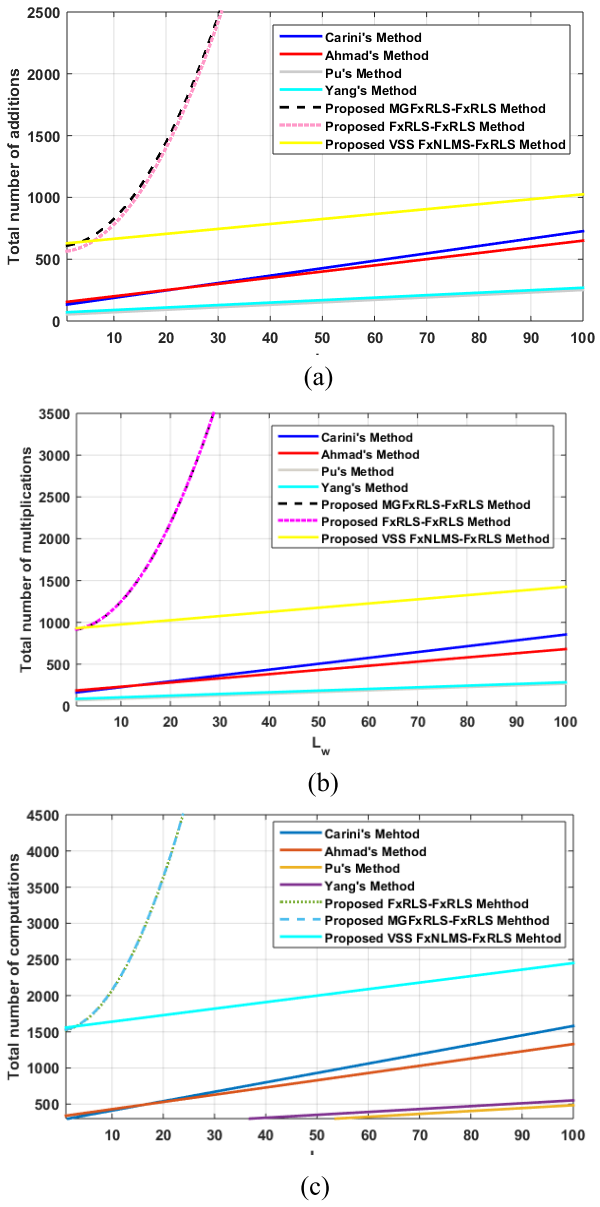

FIGURE 6. Complexity comparison plots of the investigated and proposed algorithms (a) Number of additions (b) Number of multiplications (c) Total number of computations.

Fig.8 (a-c) shows the comparison of mean noise reduction, vibration reduction, and relative modeling error of various existing techniques, respectively. Fig.7 (a) depicts that *MNR* curve of Carini's method shows the fastest convergence at n = 5400 and reaches a minimum steady-state value of 0.24 *dB* as compared to other investigated algorithms. In Fig 7(b), Carini's method also exhibits the fastest growth at $n = 3400$ with respect to vibration reduction and achieves the highest value of 19 *dB*. Henceforth, it can be concluded that Carini's method is the most efficient concerning mean noise and vibration reduction amongst all reported methods in the presence of IN and stationary acoustic paths. However, Fig.7 (c) shows that Carini *et al.*'s method shows slow convergence and does not provide the most accurate model of

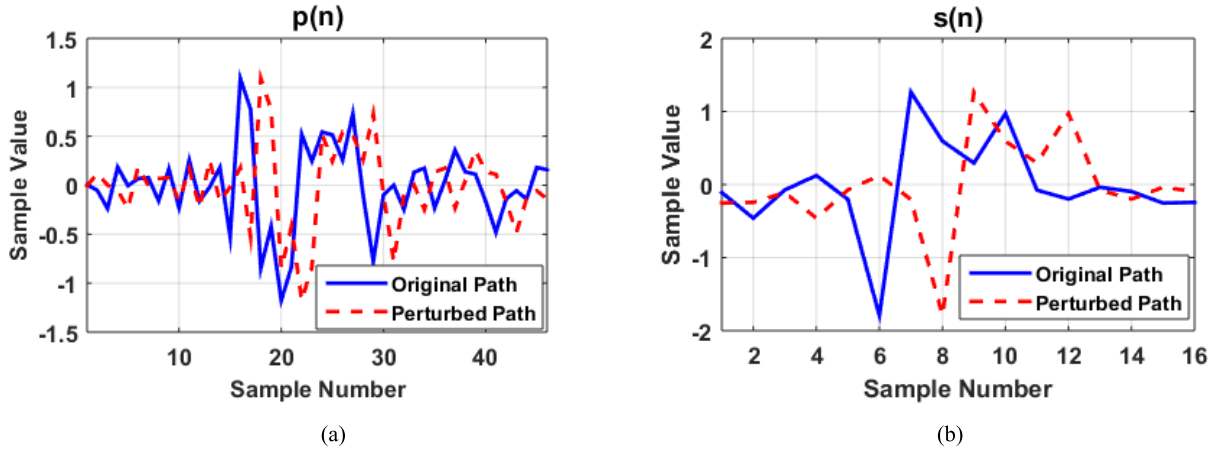

(a) (b)

FIGURE 7. Impulse response of (a) Primary path (b) Secondary path.

TABLE 7. Values of controlling parameter for existing methods.

Methods	Value of Controlling Parameter		
	Case 1	Case 2	Case 3
Erikson's Method [12]	$\mu_s = 1e-7$, $\mu_w = 1e-7$	-	-
Akhtar's method [18]	$\mu_w = 1e-8$, $\mu_{s\_min} = 1e-6$ $\mu_{s\_max} = 1e-3$, $\sigma^2_{v_{min}} = 1e-3$ $\sigma^2_{v_{max}} = 1$	-	-
Carini's Method [19]	$\hat{\lambda} = 0.7$ $D = 8$ $\lambda = 0.99$ $R = 1$ $\mu_{s\_min} = 1e-4$	$\hat{\lambda} = 0.7$ $D = 8$ $\lambda = 0.99$ $R = 1$ $\mu_{s\_min} = 1e-4$	$\hat{\lambda} = 0.7$ $D = 8$ $\lambda = 0.99$ $R = 1$ $\mu_{s\_min} = 1e-4$
Ahmed's Method [21]	$\mu_1 = 0.3$ $\mu_2 = 0.08$ $\alpha = 0.997$ $\gamma_{min} = 0.3$ $\gamma_{max} = 0.9$	$\mu_1 = 0.3$ $\mu_2 = 0.08$ $\alpha = 0.997$ $\gamma_{min} = 0.3$ $\gamma_{max} = 0.9$	$\mu_1 = 0.3$ $\mu_2 = 0.08$ $\alpha = 0.997$ $\gamma_{min} = 0.3$ $\gamma_{max} = 0.9$
Pu's Method [22]	$\mu_w = 1e-8$	-	-
Yang's Method [23]	$\mu_w = 1e-8$ $\mu_h = 1e-7$ $\alpha = 0.005$	$\mu_w = 1e-8$ $\mu_h = 1e-7$ $\alpha = 0.005$	$\mu_w = 1e-8$ $\mu_h = 1e-7$ $\alpha = 0.005$

secondary path modeling whereas, Yang and Ahmed's methods exhibit fast convergence and good modeling accuracy by achieving the lowest value of ΔS i.e., $-30\,dB$ at $n = 12000$ and $n = 6700$, respectively.

From Fig. 8, it is authenticated Erikson's, Akhtar's, and Pu's methods diverge in the presence of IN. Moreover, Carini's method gives the best reduction in noise and vibration for moderate IN whereas Ahmed's and Yang's

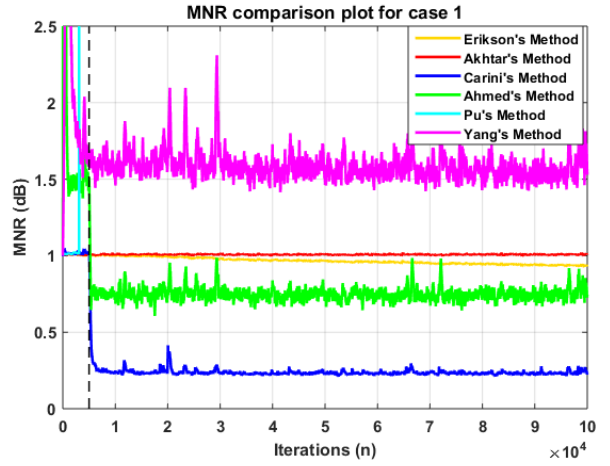

(a)

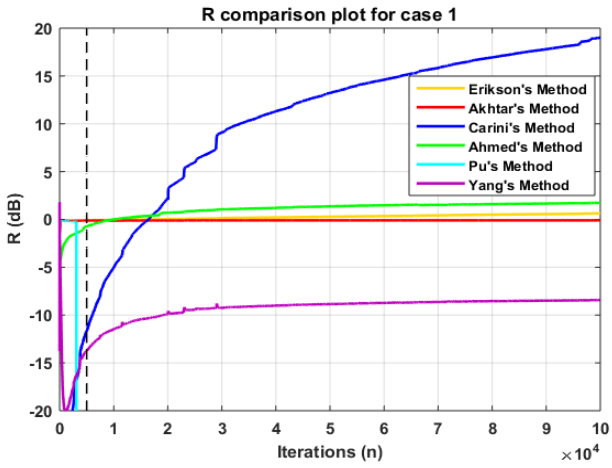

(b)

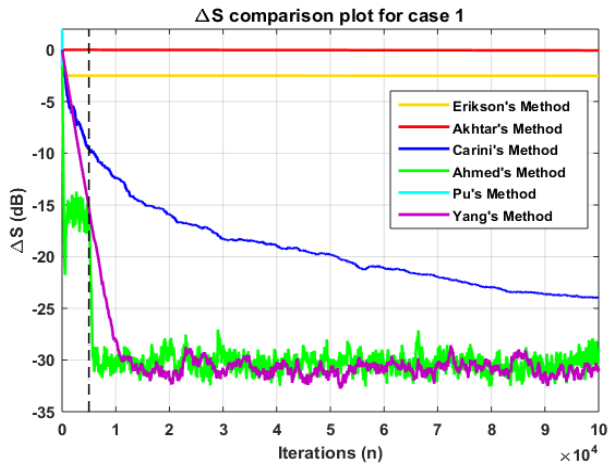

(c)

FIGURE 8. Performance evaluation of existing methods for case 1: (a) MNR (b) R (c) ΔS.

methods give the best estimate of the secondary path with the best modeling speed and accuracy. Therefore, in the next set of experiments, Carini's, Ahmed's, and Yang's methods have been selected for comparison with proposed methods in a non-stationary acoustic environment.

B. CASE 2: MODERATE IMPULSIVE INPUT ($\alpha = 1.85$) WITH NON-STATIONARY ACOUSTIC PATHS

In this case, moderate impulsive input ($\alpha = 1.85$) with non-stationary acoustic paths is considered to check the performance of existing methods of ANC system with OSPM. For this purpose, a strong perturbation is given to both primary and secondary acoustic paths by generating two sample right circular shifts at 50,000 iterations. The impulse response of perturbed primary and secondary acoustic paths is displayed in Fig. 7. The comparative results of Carini's, Ahmed's, and Yang's for time-varying acoustic paths are illustrated in Fig. 9.

From Fig. 9(a-c), it is evident that Carini's method diverges for all three performance metrics whenever a perturbation in acoustic paths is encountered. Ahmed's method shows relatively better convergence along with better noise and vibration reduction, whereas Yang's method has comparatively superior modeling accuracy. Therefore, we have selected Ahmed's and Yang's methods for further comparison with our proposed methods in non-stationary acoustic paths. The values of various controlling parameters of proposed methods for the three cases are listed in Table 8. The value of μ_h and λ is kept the same for all simulations i.e., $\mu_h = 1e-4$ and $\lambda = 0.9999$.

Fig. 10 (a-c) shows that Yang's and Ahmed's methods give slow convergence and are less robust in comparison to FxRLS family algorithms. The proposed FxRLS-FxRLS method provides good convergence as compared to Ahmed's and Yang's methods. The *MNR* of the proposed FxRLS-FxRLS method converges at around 14000 iterations, whereas relative modeling error takes almost 10000 iterations to achieve a steady-state value. The highest vibration reduction value achieved by this method is 13 dB. This method is neither robust enough nor fastest converging for non-stationary acoustic paths. The proposed MGFxRLS-FxRLS method gives better performance i.e., faster convergence, better noise reduction, good modeling accuracy and enhanced robustness than the proposed FxRLS-FxRLS method under non-stationary acoustic paths as it achieves the lowest value for *MNR* at about 6000 iterations and for ΔS, the steady-state value is achieved only within 6000 iterations. The highest vibration reduction value achieved by the proposed MGFxRLS-FxRLS method is 14.5 dB. Furthermore, although the proposed MGFxRLS-FxRLS method is giving faster convergence and improved robustness and stability than all existing algorithms. However, when compared to FxLMS variants, this improved performance is achieved at the overhead of increased computational load. The newly proposed VSS FxNLMS-FxRLS method is giving the same performance as that of the proposed MGFxRLS-FxRLS method along with the reduced computational load.

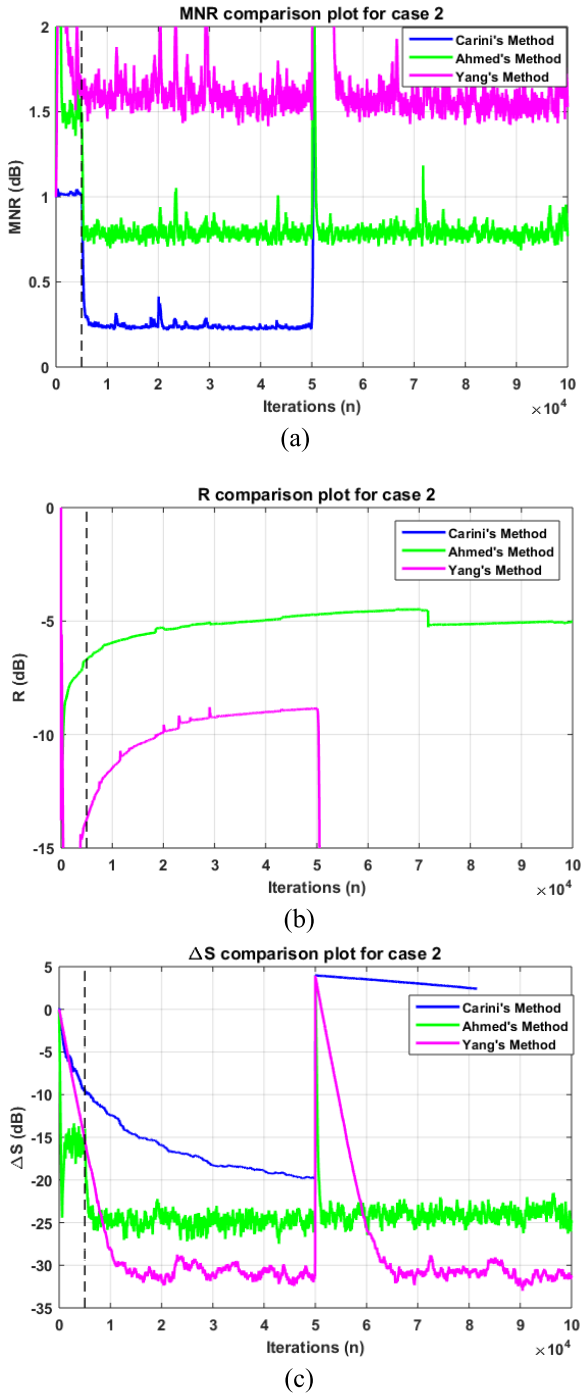

FIGURE 9. Performance evaluation with existing methods for case 2: (a) MNR (b) R (c) ΔS.

C. CASE 3: HIGH IMPULSIVE INPUT ($\alpha = 1.65$) WITH NON-STATIONARY ACOUSTIC PATHS

In this case, high impulsive input ($\alpha = 1.65$) with non-stationary acoustic paths is considered to validate the performance of investigated methods of ANC system with OSPM. For this purpose, a strong perturbation is given to truncated impulse responses of both primary and secondary acoustic paths by generating two sample right circular shifts at 50,000 iterations. The primary and secondary acoustic paths' impulse responses after perturbation are shown in Fig. 7. The comparative results of Ahmed's, Yang's, and three proposed methods for non-stationary acoustic paths are illustrated in Fig. 10-11.

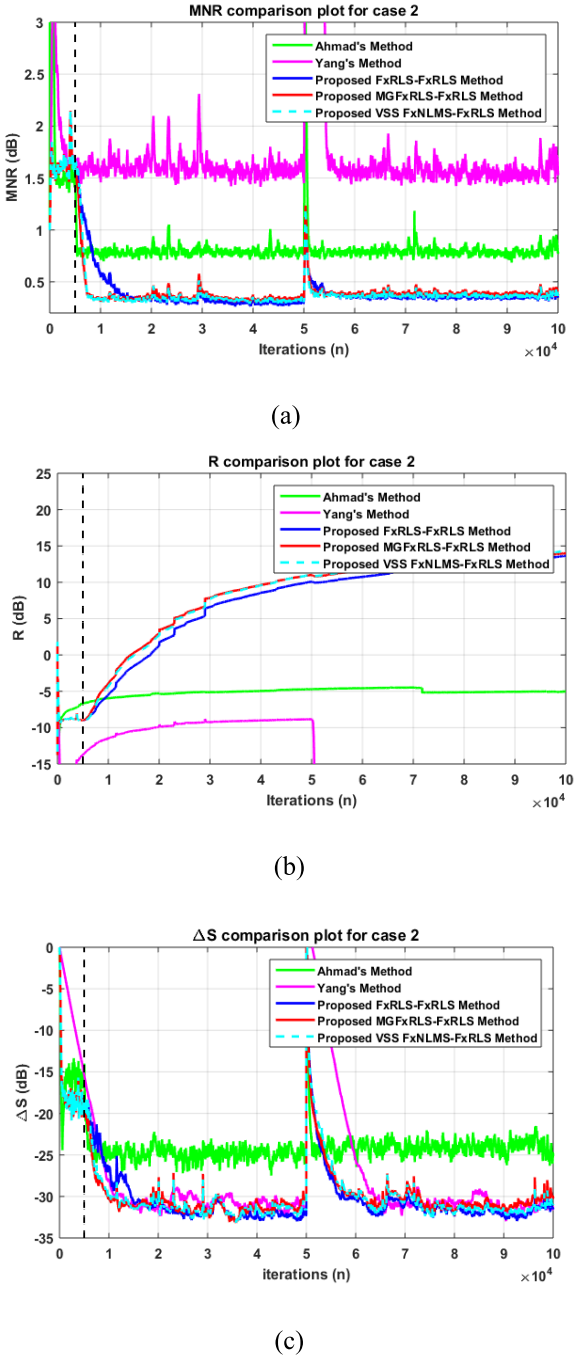

FIGURE 10. Performance evaluation of proposed methods for case 2: (a) MNR (b) R (c) ΔS.

The results from Fig. 11 (a-c) yet again substantiate the superior performance of all proposed solutions to the standard OSPM methods in terms of vibration and noise reduction, robustness, modeling accuracy, and modeling speed. As depicted in Fig. 10, the proposed FxRLS-FxRLS method is not considered stable under high IN, whereas the proposed

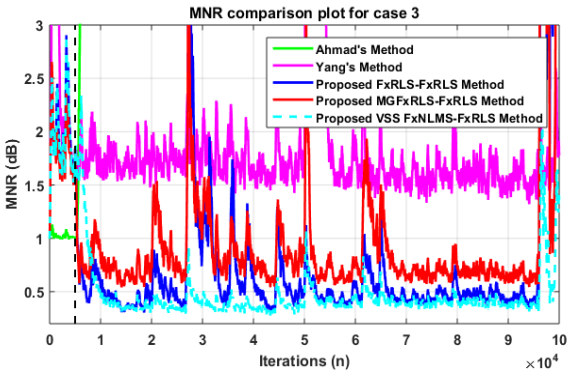

(a)

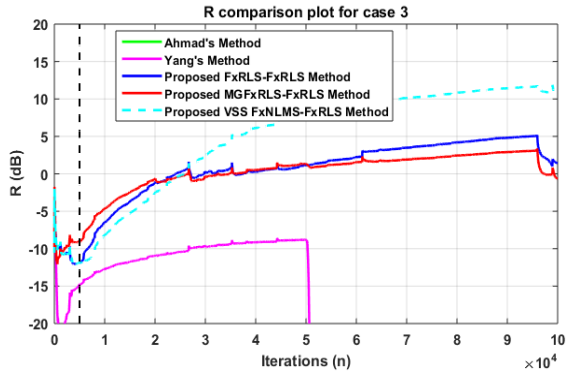

(b)

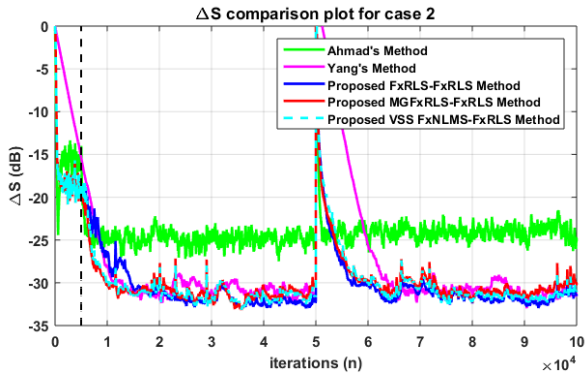

(c)

FIGURE 11. Performance comparison of proposed methods for case 3: (a) MNR (b) R (c) ΔS.

MGFxRLS-FxRLS method is relatively stable in comparison to the proposed FxRLS-FxRLS method. The proposed VSS FxNLMS-FxRLS method has even better performance than the proposed MGFxRLS-FxRLS method in terms of robustness, modeling accuracy, stability, and noise reduction. Furthermore, it is established from Table 5 that the proposed VSS FxNLMS-FxRLS method has also decreased the computational freight as compared to the proposed

TABLE 8. Values of controlling parameter of proposed methods.

Methods	Values of Controlling Parameter	
	Case 2	Case 3
Proposed FxRLS-FxRLS method	δ_1=100,000 δ_2=1000	δ_1=1000 δ_2=1000
Proposed MGFxRLS-FxRLS method	δ_1=1000 δ_2=1000	δ_1=1000 δ_2=1000
Proposed VSS FxNLMS-FxRLS method	δ_2=1000 $\hat{\lambda} = 0.9$	δ_2=1000 $\hat{\lambda} = 0.9$

FxRLS-FxRLS and proposed MGFxRLS-FxRLS methods. Hence, the proposed VSS FxNLMS-FxRLS method gives an enhanced performance with reduced complexity.

It has been observed from simulation experiments that for IN and non-varying acoustic paths Carini's method gave fast convergence best noise and vibration reduction among all existing methods of ANC with OSPM. However, this method lacked robustness as it diverges when acoustic paths are non-stationary (see Fig. 9). The proposed FxRLS-FxRLS method gave faster convergence but still lacked robustness. To achieve robustness along with the preservation of fast convergence and good modeling accuracy and modeling speed, a proposed MGFxRLS-FxRLS method is devised. This method achieved the enhanced robustness and performance but at the cost of additional computational load. The proposed VSS FxNLMS-FxRLS method which is developed to reduce the computational complexity of the proposed MGFxRLS-FxRLS method without making a compromise on system performance gives the best performance of all the existing and proposed methods as evident from Fig. 10-11.

V. CONCLUSION

We have tested active noise control (ANC) of impulsive noise (IN) with online secondary path modeling (OSPM). In this paper, three new methods are proposed using the filtered-x recursive least squares (FxRLS) family of algorithms. Simulation results illustrated that the proposed FxRLS-FxRLS method gives better convergence and modeling accuracy in comparison of filtered-x least mean square (FxLMS) family algorithms but shortages robustness in presence of non-stationary acoustic paths. To enhance the robustness, a modified gain FxRLS (MGFxRLS) based proposed MGFxRLS-FxRLS method has been devised. This method gave faster convergence with better stability and robustness than the proposed FxRLS-FxRLS method. However, FxRLS and MGFxRLS are computationally complex algorithms. To lessen the computational load the third method i.e. proposed VSS-FxNLMS-FxRLS is presented. The results proved that the proposed VSS-FxNLMS-FxRLS method achieves faster convergence, good modeling accuracy, and modeling speed with reduced computational complexity as compared to other reported and proposed methods.

REFERENCES

[1] S. M. Kuo and D. R. Morgan, *Active Noise Control Systems-Algorithms and DSP Implementation*. New York, NY, USA: Wiley, 1996.

[2] D. Yang, Y. Cheng, J. Zhu, D. Xue, G. Abt, H. Ye, and Y. Peng, "A novel adaptive spectrum noise cancellation approach for enhancing heartbeat rate monitoring in a wearable device," *IEEE Access*, vol. 6, pp. 8364–8375, 2018.

[3] C. Wu and P. Yu, "A study on active noise reduction of automobile engine compartment based on adaptive LMS algorithm," *Acoust. Aust.*, vol. 48, pp. 431–440, Aug. 2020.

[4] S. Fan, Y. Xiao, S. Fang, Y. Zhao, and X. Zhou, "Clipping noise cancellation for signal detection of GSTFIM systems," *IEEE Access*, vol. 8, pp. 33830–33837, 2020.

[5] S. J. Elliott and J. Cheer, "Modeling local active sound control with remote sensors in spatially random pressure fields," *J. Acoust. Soc. Amer.*, vol. 137, no. 4, pp. 1936–1946, 2015.

[6] Y. Tsa, H.-C. Chu, S.-H. Fang, J. Lee, and C.-M. Lin, "Adaptive noise cancellation using deep cerebellar model articulation controller," *IEEE Access*, vol. 6, pp. 37395–37402, 2018.

[7] D. Morgan, "An analysis of multiple correlation cancellation loops with a filter in the auxiliary path," *IEEE Trans. Acoust., Speech, Signal Process.*, vol. I-28, no. 4, pp. 454–467, Aug. 1980.

[8] N. Sato and T. Sone, "Influence of modeling error on noise reduction performance of active noise control systems using filtered-X LMS algorithm," *J. Acoust. Soc. Jpn., E*, vol. 17, no. 4, pp. 195–202, 1996.

[9] C. C. Boucher, S. J. Elliott, and P. A. Nelson, "Effect of errors in the plant model on the performance of algorithms for adaptive feedforward control," *IEE Proc. F (Radar Signal Process.)*, vol. 138, no. 4, pp. 313–319, Aug. 1991.

[10] M. Wu, X. Qiu, and G. Chen, "The statistical behavior of phase error for deficient-order secondary path modeling," *IEEE Signal Process. Lett.*, vol. 15, pp. 313–316, 2008.

[11] P. L. Feintuch, N. J. Bershad, and A. K. Lo, "A frequency domain model for 'filtered' LMS algorithms-stability analysis, design, and elimination of the training mode," *IEEE Trans. Signal Process.*, vol. 41, no. 4, pp. 1518–1531, Apr. 1993.

[12] L. J. Eriksson and M. C. Allie, "Use of random noise for on-line transducer modeling in an adaptive active attenuation system," *J. Acoust. Soc. Amer.*, vol. 85, no. 2, pp. 797–802, 1989.

[13] C. Bao, P. Sas, and H. Van Brussel, "Comparison of two-on-line identification algorithms for active noise control," in *Proc. 2nd Conf. Recent Adv. Active Control Sound Vib.*, 1993, pp. 38–54.

[14] S. M. Kuo and D. Vijayan, "A secondary path modeling technique for active noise control systems," *IEEE Trans. Speech Audio Process.*, vol. 5, no. 4, pp. 374–377, Jul. 1997.

[15] M. Zhang, H. Lan, and W. Ser, "Cross-updated active noise control system with online secondary path modeling," *IEEE Trans. Speech Audio Process.*, vol. 9, no. 5, pp. 598–602, Jul. 2001.

[16] M. Zhang, H. Lan, and W. Ser, "A robust online secondary path modeling method with auxiliary noise power scheduling strategy and norm constraint manipulation," *IEEE Trans. Speech Audio Process.*, vol. 11, no. 1, pp. 45–53, Jan. 2003.

[17] M. T. Akhtar, M. Abe, and M. Kawamata, "A new variable step size LMS algorithm-based method for improved online secondary path modeling in active noise control systems," *IEEE Trans. Audio, Speech, Language Process.*, vol. 14, no. 2, pp. 720–726, Mar. 2006.

[18] M. T. Akhtar, M. Abe, and M. Kawamata, "Noise power scheduling in active noise control systems with online secondary path modeling," *IEICE Electron. Exp.*, vol. 4, no. 2, pp. 66–71, 2007.

[19] A. Carini and S. Malatini, "Optimal variable step-size NLMS algorithms with auxiliary noise power scheduling for feedforward active noise control," *IEEE/ACM Trans. Audio, Speech, Language Process.*, vol. 16, no. 8, pp. 1383–1395, Nov. 2008.

[20] P. Davari and H. Hassanpour, "A new online secondary path modelling method for feedforward active noise control systems," in *Proc. IEEE Int. Conf. Ind. Technol.*, Apr. 2008, pp. 1–6.

[21] S. Ahmed, M. T. Akhtar, and X. Zhang, "Robust auxiliary-noise-power scheduling in active noise control systems with online secondary path modeling," *IEEE/ACM Trans. Audio, Speech, Language Process.*, vol. 21, no. 4, pp. 749–761, Apr. 2013.

[22] Y. Pu, F. Zhang, and J. Jiang, "A new online secondary path modeling method for adaptive active structure vibration control," *Smart Mater. Struct.*, vol. 23, no. 6, Jun. 2014, Art. no. 065015.

[23] T. Yang, L. Zhu, X. Li, and L. Pang, "An online secondary path modeling method with regularized step size and self-tuning power scheduling," *J. Acoust. Soc. Amer.*, vol. 143, no. 2, pp. 1076–1084, Feb. 2018.

[24] M. Shao and C. L. Nikias, "Signal processing with fractional lower order moments: Stable processes and their applications," *Proc. IEEE*, vol. 81, no. 7, pp. 986–1010, Jul. 1993.

[25] S. Haykin, *Adaptive Filter Theory*. Upper Saddle River, NJ, USA: Prentice-Hall, 2002.

[26] A. Zeb, A. Mirza, Q. U. Khan, and S. A. Sheikh, "Improving performance of FxRLS algorithm for active noise control of impulsive noise," *Appl. Acoust.*, vol. 116, pp. 364–374, Jan. 2017.

[27] M. T. Akhtar, "Novel recursive least squares-based filtered-X adaptive algorithm developed for active control of impulsive noise sources," in *Proc. IEEE Int. Conf. Syst., Man, Cybern. (SMC)*, Oct. 2020, pp. 2359–2364.

[28] M. Bergamasco, F. Della Rossa, and L. Piroddi, "Active noise control with on-line estimation of non-Gaussian noise characteristics," *J. Sound Vib.*, vol. 331, no. 1, pp. 27–40, Jan. 2012.

[29] L. Lu, K. L. Yin, R. C. de Lamare, Z. Zheng, Y. Yu, X. Yang, and B. Chen, "A survey on active noise control in the past decade–Part I: Linear systems," *Signal Process.*, vol. 183, Jun. 2021, Art. no. 108039.

[30] L. Lu, K. L. Yin, R. C. de Lamare, Z. Zheng, Y. Yu, X. Yang, and B. Chen, "A survey on active noise control in the past decade–Part II: Nonlinear systems," *Signal Process.*, vol. 181, Apr. 2020, Art. no. 107929.

[31] A. Naeimi Sadigh, A. H. Taherinia, and H. Sadoghi Yazdi, "Analysis of robust recursive least squares: Convergence and tracking," *Signal Process.*, vol. 171, Jun. 2020, Art. no. 107482.

[32] M. S. Aslam, P. Shi, and C.-C. Lim, "Robust active noise control design by optimal weighted least squares approach," *IEEE Trans. Circuits Syst. I, Reg. Papers*, vol. 66, no. 10, pp. 3955–3967, Oct. 2019.

[33] G. Akgün, H. ul Hasan Khan, M. Hebaish, and D. Gohringer, "System identification using LMS, RLS, EKF and neural network," in *Proc. IEEE Int. Conf. Veh. Electron. Saf. (ICVES)*, Sep. 2019, pp. 1–6.

[34] R. M. Reddy, I. M. S. Panahi, R. Briggs, and E. Perez, "Performance comparison of FXRLS, FXAPA and FXLMS active noise cancellation algorithms on an fMRI bore test-bed," in *Proc. IEEE Dallas Eng. Med. Biol. Workshop*, Nov. 2007, p. 130.